Since January 2020 Elsevier has created a COVID-19 resource centre with free information in English and Mandarin on the novel coronavirus COVID-19. The COVID-19 resource centre is hosted on Elsevier Connect, the company's public news and information website.

VIROLOGY 242, 288–302 (1998)
ARTICLE NO. VY979010

Processing of the Coronavirus MHV-JHM Polymerase Polyprotein: Identification of Precursors and Proteolytic Products Spanning 400 Kilodaltons of ORF1a

Jennifer J. Schiller, Amornrat Kanjanahaluethai, and Susan C. Baker[1]

Department of Microbiology and Immunology, Loyola University of Chicago, Stritch School of Medicine, 2160 South First Avenue, Maywood, Illinois 60153

Received September 19, 1997; returned to author for revision October 24, 1997; accepted December 19, 1997

The replicase of mouse hepatitis virus strain JHM (MHV-JHM) is encoded by two overlapping open reading frames, ORF1a and ORF1b, which are translated to produce a 750-kDa precursor polyprotein. The polyprotein is proposed to be processed by viral proteinases to generate the functional replicase complex. To date, only the MHV-JHM amino-terminal proteins p28 and p72, which is processed to p65, have been identified. To further elucidate the biogenesis of the MHV-JHM replicase, we cloned and expressed five regions of ORF1a in bacteria and prepared rabbit antisera to each region. Using the immune sera to immunoprecipitate radiolabeled proteins from MHV-JHM infected cells, we determined that the MHV-JHM ORF1a is initially processed to generate p28, p72, p250, and p150. Pulse–chase analysis revealed that these intermediates are further processed to generate p65, p210, p40, p27, the MHV 3C-like proteinase, and p15. A putative replicase complex consisting of p250, p210, p40, p150, and a large protein (>300 kDa) coprecipitate from infected cells disrupted with NP-40, indicating that these proteins are closely associated even after initial proteolytic processing. Immunofluorescence studies revealed punctate labeling of ORF1a proteins in the perinuclear region of infected cells, consistent with a membrane-association of the replicase complex. Furthermore, *in vitro* transcription/translation studies of the MHV-JHM 3Cpro and flanking hydrophobic domains confirm that 3C protease activity is significantly enhanced in the presence of canine microsomal membranes. Overall, our results demonstrate that the MHV-JHM ORF1a polyprotein: (1) is processed into more than 10 protein intermediates and products, (2) requires membranes for efficient biogenesis, and (3) is detected in discrete membranous regions in the cytoplasm of infected cells.

INTRODUCTION

Mouse hepatitis virus strain JHM (MHV-JHM) is a member of the positive strand RNA virus family *Coronaviridae,* in the new order *Nidovirales* (Cavanagh, 1997; de Vries *et al.,* 1997). *Nido,* Latin for "nest," was chosen for this order since the two virus families in the order, the *Coronaviridae* and *Arteriviridae,* synthesize a 3′-nested set of mRNAs. Furthermore, the nested set of mRNAs is generated by an unusual discontinuous transcription process in which a short leader RNA sequence and the body sequence of the mRNA are joined (Baric *et al.,* 1983; Lai *et al.,* 1994; Spaan *et al.,* 1983; van der Most and Spaan, 1995). The mechanism by which this discontinuous transcription occurs to generate the nested set of mRNAs is controversial (Jeong and Makino, 1994; Sawicki and Sawicki, 1990; Sethna *et al.,* 1989; van Marle *et al.,* 1995; Zhang and Lai, 1995). However, it is clear that the enzyme that mediates discontinuous transcription is the viral RNA-dependent RNA polymerase, or replicase. By understanding how this replicase is generated and functions throughout the infection cycle, we may gain insight regarding how it mediates the unusual mechanism of discontinuous RNA synthesis.

The MHV-JHM replicase is encoded at the 5′-end of the positive strand RNA genome in a region designated gene 1. Gene 1 encompasses 21.7 kb of the almost 32-kb viral genome and contains two overlapping open reading frames: ORF1a (13.6 kb) and ORF1b (8.1 kb) (Lee *et al.,* 1991; Pachuk *et al.,* 1989). These two open reading frames are joined by a −1 ribosomal frameshift that occurs during translation of gene 1, leading to the generation of a 750-kDa replicase polyprotein (Brierley *et al.,* 1987; Lee *et al.,* 1991). This large polyprotein is thought to be processed by viral proteinases to generate the mature, functional replicase complex.

Within gene 1 of MHV there are three predicted proteinase domains, two of which are papain-like cysteine proteinase domains (PCP-1 and PCP-2) and a third which is poliovirus 3C-like (3Cpro) (Gorbalenya *et al.,* 1989; Lee *et al.,* 1991). To date, only PCP-1 and 3Cpro of MHV have been demonstrated to have activity (Baker *et al.,* 1989, 1993; Bonilla *et al.,* 1997; Lu *et al.,* 1995). The first protein to be processed from the replicase polyprotein, p28, is cleaved from the amino-terminus of the ORF1a polyprotein precursor by the PCP-1 proteinase (Baker *et al.,* 1989; Denison and Perlman, 1987). This is followed by processing of the adjacent 72-kDa protein and its cleav-

[1] To whom correspondence and reprint requests should be addressed. Fax: (708) 216-9574. E-mail: sbaker@luc.edu.

0042-6822/98 $25.00

TABLE 1

Primers Used for PCR Amplification of MHV-JHM ORF1a Domains

Primer name	Oligonucleotide sequence (5′ to 3′)[a]	Nucleotides of ORF1a[b]	Polarity	Domain generated
FP22	TATCTAGAAGGCTGTTGTAAGC	2563–2576	+	D3
FP23	TGAAGCTTCAGTTGCCTTGACC	3313–3326	−	
FP1	TATCTAGACGTGTTTTTCTATGGAGACG	3847–3866	+	D5
B11	ACCACCGGTAGACTCATAGC	4374–4393	−	
FP28	TATCTAGATACGTATAACAAGCAGGAGG	8671–8690	+	D10
FP29	TGAAGCTTTGCAGTAGGTCATGGAGCGC	9376–9395	−	
FP2	TATCTAGAAGTGAAGATGGTGTCC	10231–10246	+	D12
FP3	TGAAGCTTTATGGCTGCTACGC	10612–10625	−	
FP12	ATTCTAGACTCTGCAAATAGGC	12811–12824	+	D15
FP13	TGAAGCTTTGACTGAAACTGGG	13584–13597	−	
B151	GCTCTAGAATAATGGCCTTTGGTGACTACAC	9650–9666	+	3Cpro
B158	ATGAATTCTCATGCAATGTGCAAGTGC	12049–12064	−	
B153[c]	TTGGATCCAGAGGTTCTGTAGGG	10649–10669	+	mut3Cpro
B158	ATGAATTCTCATGCAATGTGCAAGTGC	12049–12064	−	

[a] Underlined nucleotides refer to sequences added for cloning purposes.
[b] Nucleotides numbered according to Lee *et al.* (1991) as modified by Bonilla *et al.* (1994).
[c] Nucleotides in bold indicate base mismatches incorporated into the primer sequence which result in a change in the coding sequence from cysteine to arginine. This amplified product was ligated into the *Bam*HI–*Eco*RI site of pET-3Cpro as described under Materials and Methods.

age to a 65-kDa protein in MHV-JHM (Gao *et al.,* 1996). For MHV-A59, p65 has been detected, followed by a 290-kDa protein which is processed into p240 and p50 (Denison *et al.,* 1992, 1995). Two proteins of 27 and 29 kDa, representing the 3Cpro, have also been detected from MHV-A59-infected cells, but no precursor to this protein was detected (Lu *et al.,* 1996; Piñón *et al.,* 1997). To determine the biogenesis of the MHV-JHM replicase, we sought to identify ORF1a precursors and products from virus-infected cells. Elucidation of the steps in the biogenesis of the coronavirus polymerase from its polyprotein precursor to its functional subunits will aid our understanding of coronavirus transcription, replication, and RNA recombination and may provide valuable insight into targets for anti-viral drug design.

For this study, we prepared rabbit antisera against five regions within MHV-JHM ORF1a and determined that at least 10 intermediates and products are generated by proteolytic processing of the precursor replicase polyprotein. Using pulse–chase analyses, we determined precursor–product relationships between several of these proteins. In addition, we provide immunofluorescence and *in vitro* processing data to support the hypothesis that the MHV-JHM replicase is a cytoplasmic, membrane-associated enzyme complex.

RESULTS

Identification of MHV-JHM polymerase gene products

To elucidate the biogenesis of the coronavirus RNA-dependent RNA polymerase, we generated polyclonal antisera against five regions of MHV-JHM ORF1a. To prepare each antigen of interest, domains within gene 1 were RT-PCR amplified from total RNA of MHV-JHM-

TABLE 2

Antisera Generated Against GST/MHV-JHM-ORF1a Fusion Proteins

Antiserum	Number of amino acids in ORF1a antigen	Primers used for PCR amplification[a]	Amino acid position in the ORF1a protein[b]	ORF1a products detected by immunoprecipitation
αD3	254	FP22–FP23	784–1037	p250, p210, p72, p65[c]
αD5	154	FP1–B11	1212–1365	p250, p210[c]
αD10	241	FP28–FP29	2820–3060	p250, p210[c]
αD12	131	FP2–FP3	3340–3470	p150, p27
αD15	262	FP12–FP13	4200–4461	p150, p15

[a] See Table 1 for details regarding each primer.
[b] Amino acids numbered according to Lee *et al.* (1991) as modified by Bonilla *et al.* (1994).
[c] p40 detected using lysis method B with αD3, αD5, and αD10 antisera (see Fig. 4).

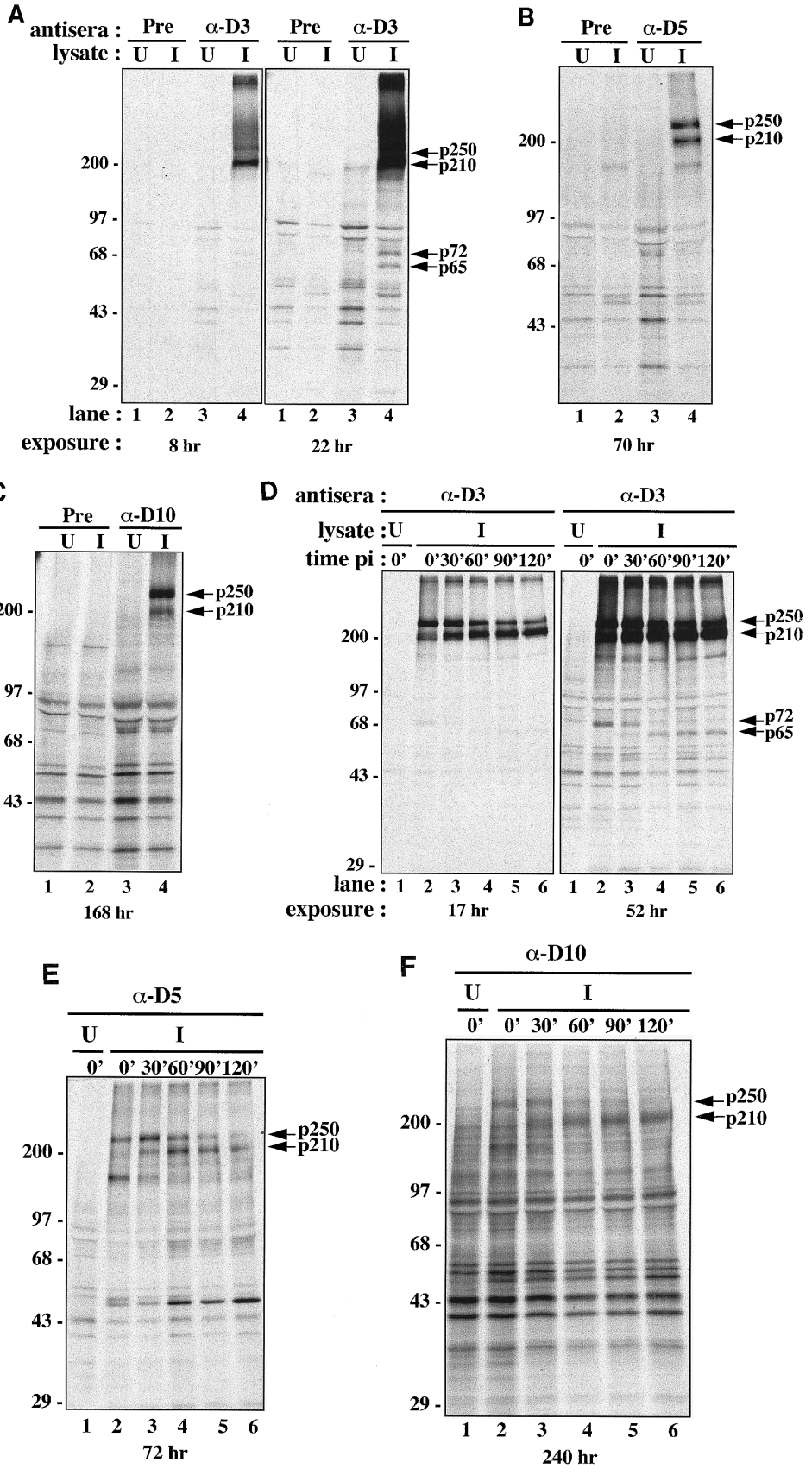
A
antisera : Pre α-D3 Pre α-D3
lysate : U I U I U I U I
200 -
97 -
68 -
43 -
29 -
p250
p210
p72
p65
lane : 1 2 3 4 1 2 3 4
exposure : 8 hr 22 hr
B
Pre α-D5
U I U I
200 -
97 -
68 -
43 -
p250
p210
1 2 3 4
70 hr
C
Pre α-D10
U I U I
200 -
97 -
68 -
43 -
p250
p210
1 2 3 4
168 hr
D
antisera : α-D3 α-D3
lysate : U I U I
time pi : 0' 0'30'60' 90'120' 0' 0' 30'60'90'120'
200 -
97 -
68 -
43 -
29 -
p250
p210
p72
p65
lane : 1 2 3 4 5 6 1 2 3 4 5 6
exposure : 17 hr 52 hr
E
α-D5
U I
0' 0' 30'60'90'120'
200 -
97 -
68 -
43 -
29 -
p250
p210
1 2 3 4 5 6
72 hr
F
α-D10
U I
0' 0' 30' 60' 90' 120'
200 -
97 -
68 -
43 -
29 -
p250
p210
1 2 3 4 5 6
240 hr

infected cells (see Tables 1 and 2), cloned in frame with glutathione *S*-transferase (GST) in the bacterial expression vector pGEX-KG, and expressed as described under Materials and Methods. Affinity-column-purified GST-fusion proteins were used for rabbit immunizations, and sera were collected 10–14 days following each injection. Antibody titer was determined by ELISA assay to GST antigen alone and GST-ORF1a fusion proteins. Final bleed antisera had titers greater than 80,000 against GST-ORF1a fusion proteins.

To identify MHV-JHM ORF1a products, immunoprecipitations from MHV-JHM-infected DBT cell lysates were performed using the D3, D5, and D10 antisera. The fusion proteins used to generate these antisera cover amino acids 784–1037, 1212–1365 and 2820–3060, respectively (Table 2). Immunoprecipitations with these antisera led to the identification of two high-molecular-weight proteins with apparent migrations of 250 and 210 kDa (Figs. 1 A–1C, lane 4). Longer exposure of the anti-D3 immunoprecipitation revealed proteins of 72 and 65 kDa (Fig. 1A, lane 4), confirming our earlier report of these products (Gao *et al.,* 1996). In addition, we noted proteins with apparent migrations of 180 and 50 kDa which are nonspecifically recognized by all preimmune and immune sera from infected cell lysates. These bands likely reflect some nonspecific immunoprecipitation of the highly abundant spike (180 kDa) and nucleocapsid (50 kDa) proteins produced during viral replication, as has been previously reported (Denison *et al.,* 1992, 1995). Taken together, the immunoprecipitation results suggest that p250 and p210 may be co-amino terminal (as both are precipitated by anti-D3, which extends only 14.2 kDa into the predicted p250 region), and both proteins extend to at least aa 2820 (as both are precipitated by anti-D10).

To study the synthesis and processing of p250 and p210 *in vivo,* pulse–chase analyses were performed (Figs. 1D–1F). MHV-JHM infected cells were pulsed with [^{35}S]methionine for 30 min, washed with PBS, chased with unlabeled media, and lysed as described under Materials and Methods. Immunoprecipitation of these lysates with anti-D3, anti-D5, and anti-D10 sera revealed a gradual decline in the intensity of p250 and concomitant increase in the intensity of p210, suggesting that p250 and p210 have a precursor–product relationship. We also expected to find a protein of approximately 40 kDa which would represent the remaining cleavage product of p250. However, we have been unable to detect p40 using this method. Therefore, we cannot yet definitively conclude whether p210 is co-amino- or co-carboxy-terminal with p250. Amino-terminal sequencing of p250 and p210 will be required to determine if they are truly co-amino-terminal, and at which precise amino acid they begin. To date, we have been unable to purify sufficient quantities of these proteins for amino-terminal sequencing studies.

The detection of some unprocessed p250 even 120 min into the chase (Figs. 1D–1F, lane 6) suggests that the cleavage of p250 to p210 likely occurs slowly and post-translationally. This is in contrast to the rapid cleavage of the amino-terminal product of the polymerase polyprotein, p28, which likely occurs cotranslationally and *in cis* (Denison and Perlman, 1987; Gao *et al.,* 1996), although it has been recently shown that the cleavage can also be mediated *in trans in vitro* using an internal deletion construct of the 5′ end of the MHV-A59 ORF1a (Bonilla *et al.,* 1997). The differences in the rates of processing may have important implications on replicase assembly and function (see Discussion).

Comparison of MHV-JHM and MHV-A59 ORF1a gene products

Two high molecular mass proteins, p290 and p240, have previously been reported as ORF1a cleavage products of MHV-A59 (Denison *et al.,* 1992, 1995). To determine if the MHV-JHM ORF1a processing is distinct from MHV-A59, we analyzed radiolabeled A59 and JHM lysates by immunoprecipitation with anti-D3 serum and SDS–PAGE (Fig. 2A). As seen in lanes 5 and 6, the high molecular mass proteins from both virus strains migrate identically under denaturing conditions in a 5–15% gradient SDS–polyacrylamide gel. According to our molecular mass determinations (see Materials and Methods), these proteins migrate with apparent masses of 250 and 210 kDa. Furthermore, these molecular mass estimates are consistent with the expected molecular mass calculated for the region bounded by p72 and the downstream protein p150 described below (see Fig. 7 and Table 3). Interestingly, the p72 protein appears to be unique to the MHV-JHM strain. Alignment of amino acids surrounding the p65 and p72 cleavage sites indicates that the p65 cleavage

FIG. 1. Detection of MHV-JHM ORF1a gene products by immunoprecipitation with specific antisera. (A, B, and C) Mock-infected and MHV-JHM infected DBT cells were labeled with [^{35}S]methionine from 6.0 to 7.5 h p.i. and lysed in buffer A, as described under Materials and Methods. Viral proteins were immunoprecipitated from lysates of mock-infected (lanes 1 and 3) and JHM-infected (lanes 2 and 4) cells using preimmune sera (lanes 1 and 2) and the indicated immune sera (lanes 3 and 4). Proteins p250, p210, p72, and p65 found only in infected cell lysates with immune sera are indicated by arrows. (D, E, and F) Pulse–chase analyses indicating precursor–product relationships between proteins. Mock-infected and JHM-infected cells were labeled with [^{35}S]methionine from 6.0 to 6.5 h p.i., washed with normal media, and then chased for the indicated periods of time in media containing excess cold methionine before lysis in buffer A and immunoprecipitation as described above. U, uninfected cell lysates; I, infected cell lysates. All samples were analyzed by electrophoresis in 5–15% gradient SDS–PAGE gels and visualized by fluorography. Molecular mass markers are labeled in kilodaltons on the left of each gel. Exposure lengths are indicated below each gel.

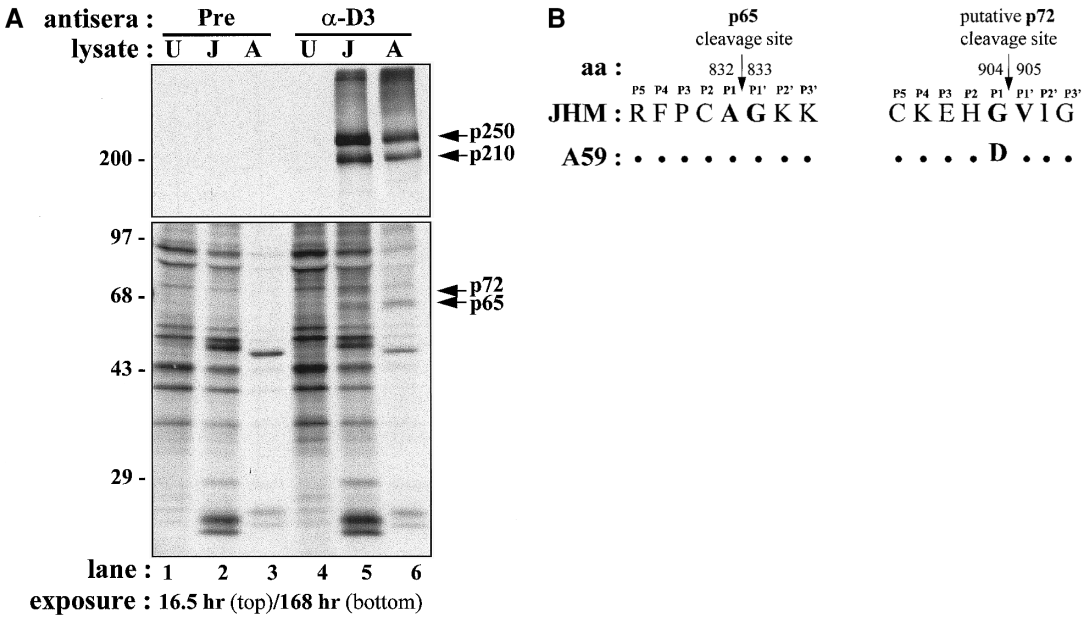

FIG. 2. Direct comparison of high molecular mass ORF1a proteins from MHV strains JHM and A59. (A) Immunoprecipitations were performed as described in the legend to Fig. 1, using both preimmune and anti-D3 immune sera. The top half of the Fig. shows a short (16.5 h) exposure, and the bottom half a longer (168 h) exposure of the same gel. U, uninfected cell lysates; J, JHM-infected cell lysates; A, A59-infected cell lysates. Proteins p250, p210, and p65 are detected in JHM and A59 lysates (lanes 5 and 6), whereas p72 is detected only in JHM lysates (lane 5). Molecular mass markers are indicated on the left of the gel, and exposure lengths are indicated below. (B) Comparison of JHM and A59 p65 and putative p72 cleavage sites. Amino acids flanking the cleavage sites are depicted in bold; dots indicate amino acid identity between virus strains.

site is identical in the two strains, whereas there is one potentially significant difference at the P1 position of the predicted p72 cleavage site (a Gly to Asp substitution; see Fig. 2B). This substitution may prevent recognition of this cleavage site in the A59 ORF1a polyprotein and therefore explain the absence of the p72 product in A59-infected cells.

Identification of MHV-JHM 3Cpro and its precursor polyprotein

All coronavirus genomes studied to date encode a poliovirus 3C-like proteinase domain (3Cpro) (Bonilla *et al.,* 1994; Boursnell *et al.,* 1987; Eleouet *et al.,* 1995; Gorbalenya *et al.,* 1989; Herold *et al.,* 1993; Lee *et al.,* 1991). For MHV-

TABLE 3

Comparison of Observed and Predicted Molecular Masses for MHV-JHM ORF1a Products

Observed molecular mass of ORF1a proteins (kDa)	Predicted amino acids in the ORF1a polyprotein[a]	Molecular mass of predicted regions (kDa)
28	Met (1)–Gly(247)[b]	27.5
72	Val (248)–Gly (904)	73.0
65	Val (248)–Ala(832)[c]	65.0
—[d]	Gly (833)–Gly (904)	7.9
250	Val (905)–Gly(3126)	246.7
150	Ala (3127)–Val(4474)	150.5
27	Ser(3337)[e]–Glu(3639)	33.2
500-kDa ORF1a polyprotein[f] (p28 + p72 + p250 + p150)	Met (1)–Val(4474)	497.6

[a] Amino acids numbered according to Lee *et al.* (1991) as modified by Bonilla *et al.* (1994).
[b] p28 cleavage site as determined by Dong and Baker (1994) and Hughes *et al.* (1995).
[c] p65 cleavage site as determined by Bonilla *et al.* (1997).
[d] Protein product predicted but not observed.
[e] p27 amino-terminal cleavage site as determined by Lu and Denison (1997).
[f] The predicted uncleaved product is not observed because it is cleaved cotranslationally.

A59, this domain spans amino acids 3334–3636 (corresponding to amino acids 3337–3639 of MHV-JHM). For the coronaviruses MHV-A59, avian infectious bronchitis virus (IBV) and human coronavirus (HCV-229E), this domain has been shown to have protease activity when translated *in vitro,* purified from virus-infected cells, or expressed in bacteria and purified (Lu *et al.,* 1995, 1996; Seybert *et al.,* 1997; Tibbles *et al.,* 1996; Ziebuhr *et al.,* 1995). The catalytic cysteine and histidine residues of the MHV-A59 and IBV proteases have been identified (Liu and Brown, 1995; Lu and Denison, 1997; Lu *et al.,* 1995), and the 3Cpro domain was detected by immunoprecipitation from MHV-A59-infected cell lysates in two different reports as a 27- or 29-kDa protein (Lu *et al.,* 1996; Piñón *et al.,* 1997). To identify the MHV-JHM 3Cpro, we prepared the fusion protein antiserum D12. The D12 domain is located within the 3C protease, specifically covering the catalytic histidine residue but not the cysteine residue (amino acids 3340–3470).

Immunoprecipitation with anti-D12 serum from MHV-JHM-infected cell lysates identified proteins of 27 and 150 kDa on 5–15% gradient SDS–PAGE gels (Fig. 3A, lane 4). Pulse–chase analysis with anti-D12 serum suggests a precursor and product relationship between p150 and p27, as reflected by the appearance of p27 30 min into the chase, and the concomitant decrease in intensity of p150 (Fig. 3C). This result is consistent with proteolytic cleavages mediated by 3Cpro occurring at Gln/Ser cleavage sites upstream and downstream of the 3Cpro catalytic center, as has been reported for MHV-A59 (Lu *et al.,* 1996). The detection of p150 is the first report of a precursor to 3Cpro. We propose that the p150 extends from a putative cleavage site upstream of the hydrophobic domain termed MP1 (Gorbalenya *et al.,* 1989; Lee *et al.,* 1991) to the end of ORF1a (Val 4474). The predicted molecular weight for this region is 150.5 kDa, similar to the apparent molecular weight of 150 kDa on SDS–PAGE gels (Table 3).

Immunoprecipitations of JHM-infected cell lysates with antiserum D15, directed against amino acids 4200–4461 near the carboxy-terminal region of ORF1a further support this hypothesis. The D15 antiserum immunoprecipitates a 150-kDa protein that decays with kinetics identical to those seen in the anti-D12 pulse–chase (Figs. 3B and 3D). To detect lower-molecular-weight cleavage products of p150, we analyzed the products by 15% SDS–PAGE (Fig. 3E). After prolonged exposure, we detected a product of 15 kDa which accumulates during the chase period. The p15 likely represents the carboxy-terminal or penultimate cleavage product of MHV-JHM ORF1a.

Effect of lysis conditions on detection of MHV-JHM ORF1a gene products

While working to optimize the conditions for immunoprecipitation of MHV-JHM ORF1a gene products, we found that the conditions used to prepare the cell lysates were critical for the detection of all MHV-JHM ORF1a products. We routinely use highly denatured total cell lysates (prepared using lysis buffer A as described under Materials and Methods) for immunoprecipitations. As shown above (Fig. 1), these conditions facilitate specific detection of MHV-JHM ORF1a gene products. Interestingly, when cell lysates were prepared using NP-40 lysis followed by isolation of postnuclear supernatants (lysis buffer B, see Materials and Methods), we detected coprecipitation of viral proteins, indicating that these proteins likely reside in the cell as a complex. Under these conditions, all five antisera described above precipitate viral proteins of >300 kDa, p250, p210, and p150 (Fig. 4). A protein of approximately 40 kDa is also detected using the anti-D3, anti-D5, and anti-D10 sera. In pulse–chase analyses of NP-40 lysates with these same three antisera, p40 is seen to accumulate during the chase concomitant with the increase in p210 and decrease in p250 intensities (data not shown). This viral p40 likely represents the additional cleavage product generated when p250 is cleaved to generate p210. Since neither the anti-D3 nor anti-D10 serum specifically immunoprecipitates this product, it is unclear if p40 represents the amino- or carboxy-terminal cleavage product of p250. The large (>300 kDa) protein likely represents an ORF1a/ORF1b polyprotein generated by ribosomal frameshifting during translation. In addition to the high-molecular-weight proteins, some specific products are also detected: p65 using anti-D3 (Fig. 4, lane 2), p27 using anti-D12 (lane 8), and p15 using anti-D15 (lane 10). The specific precipitation of the lower molecular-weight proteins demonstrates the specificity of the antisera. The coprecipitation of the high molecular weight proteins under these conditions is consistent with the hypothesis that the MHV polymerase exists as a complex of ORF1a/ORF1b cleavage products *in vivo.*

Detection of MHV-JHM ORF1a proteins by immunofluorescence

To determine the intracellular localization of MHV-JHM ORF1a proteins, immunofluorescence studies were performed. DBT cells were infected with MHV-JHM, fixed with formaldehyde at 5.5–6.0 h after infection, and incubated with specific antisera as described under Materials and Methods. MHV ORF1a products were detected using anti-D3 and anti-D12 antisera (Fig. 5). Both antisera revealed a similar, and somewhat polar, punctate staining pattern in the perinuclear region of infected cells. This pattern is consistent with MHV replicase association with discrete vesicular structures in the cells. Although not all gene 1 cleavage products are predicted to contain hydrophobic domains, it is possible that strong protein–protein interactions hold the subunits together in a membrane-associated complex. The MHV ORF1a localization we see is similar to the pattern of localization

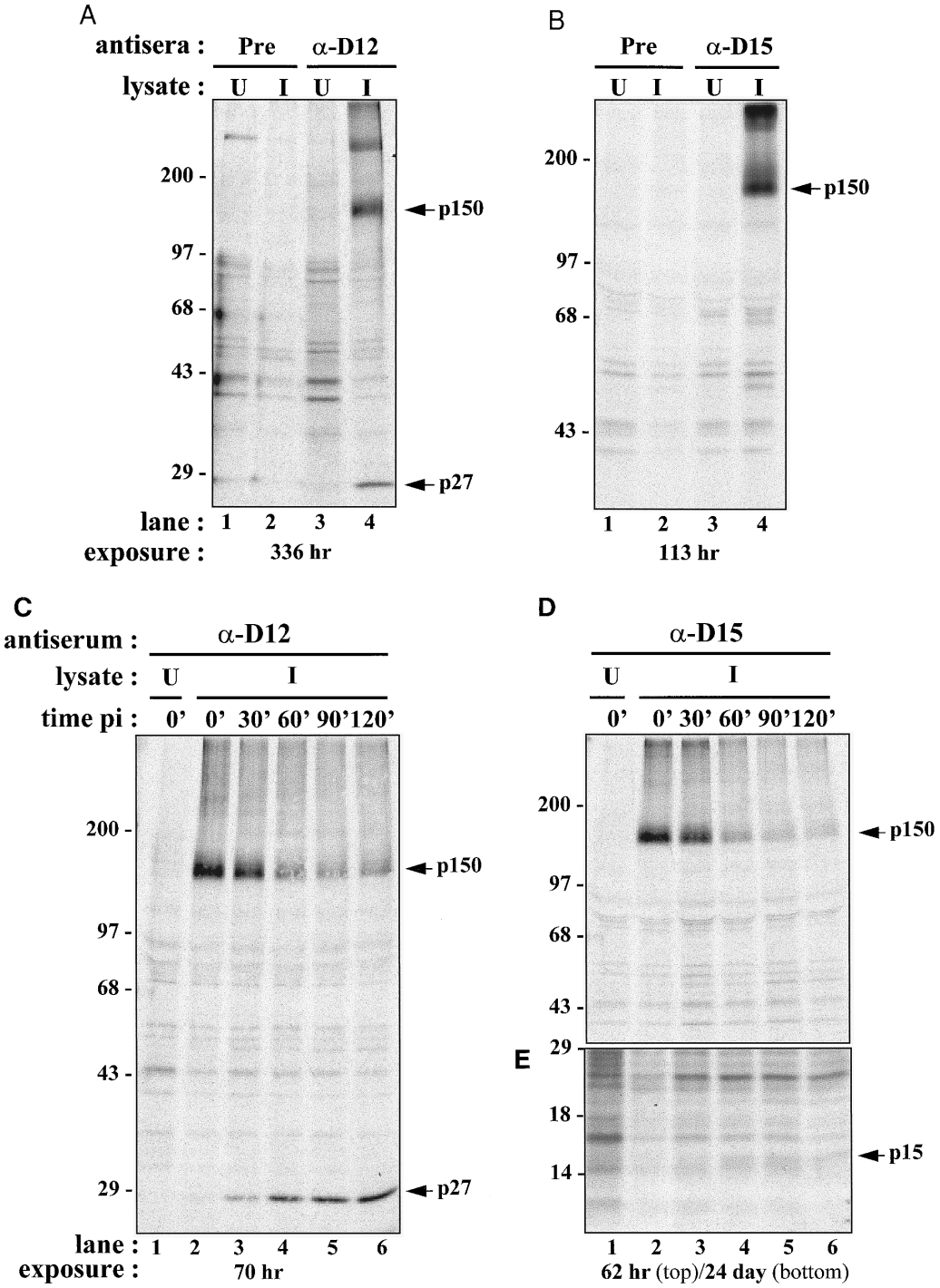

FIG. 3. Identification of the precursor and processed forms of the C-terminal region of ORF1a by immunoprecipitation with specific antisera. Immunoprecipitations and pulse–chase analyses were performed as described in the legend to Fig. 1, using anti-D12 (A and C) and anti-D15 (B, D, and E) antisera. Samples were analyzed by electrophoresis in 5–15% gradient SDS–PAGE (A–D) or 15% (E) gels and visualized by fluorography. U, uninfected cell lysates; I, infected cell lysates; pre, immunoprecipitations using preimmune sera; remaining lanes immunoprecipitated with the indicated immune sera. Proteins p150, p27 (3Cpro), and p15 are indicated by the arrows. Molecular mass markers are indicated on the left, and exposure lengths are indicated below each gel.

reported for ORF1b proteins in equine arteritis virus (EAV)-infected cells (van Dinten *et al.,* 1996). Further studies will be required to determine the precise subcellular localization site of the MHV replicase complex.

Effect of membranes on MHV-JHM 3Cpro activity

In the case of the IBV 3C-like proteinase, canine microsomal membranes (CMMs) have been shown to be

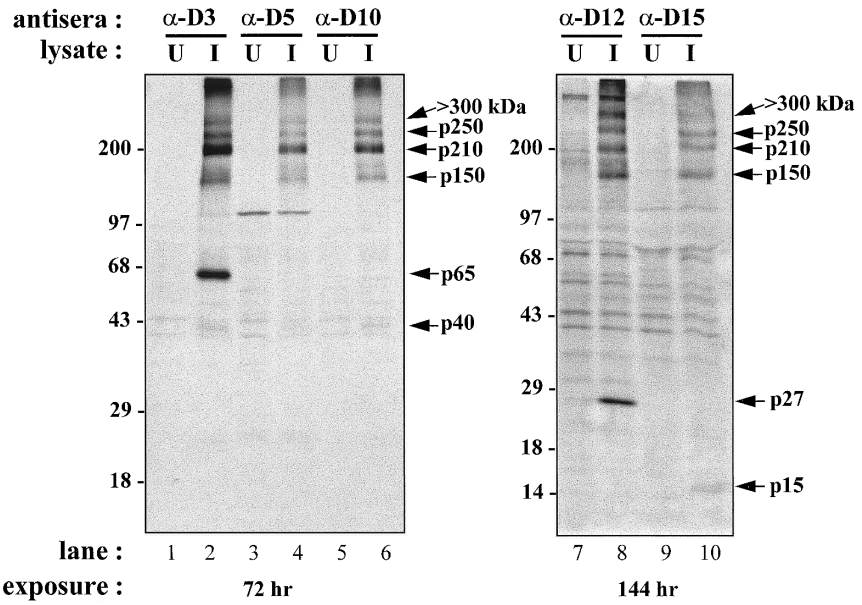

FIG. 4. Immunoprecipitation of MHV-JHM ORF1a gene products from the postnuclear supernatant of infected cells. Mock-infected and MHV-JHM infected DBT cells were labeled with [^{35}S]methionine from 6.0 to 8.0 h p.i., lysed in buffer B as described under Materials and Methods, and the postnuclear supernatants were immunoprecipitated with the indicated immune sera, electrophoresed on 5–15% gradient SDS–PAGE gels, and visualized by fluorography. U, uninfected cell lysates; I, infected cell lysates. Using this technique, proteins >300 kDa, p250, p210, and p150 are detected with all sera from infected cell lysates. In contrast, p40 is detected with anti-D3, anti-D5, and anti-D10 sera (lanes 2, 4, and 6), p65 is detected only with anti-D3 serum (lane 2), p27 is detected only with anti-D12 serum (lane 8), and p15 is detected only with anti-D15 serum (lane 10). Molecular mass markers are indicated on the left, and exposure lengths are indicated below each gel.

necessary for *in vitro* 3Cpro protease activity (Tibbles *et al.,* 1996). However, for MHV-A59 it has been demonstrated that 3Cpro (p27) does not strictly require membranes for *in vitro trans*-cleavage activity (Lu *et al.,* 1996), but that it does require membranes for efficient activity if major portions of the flanking hydrophobic domains are present in the expression constructs (Piñón *et al.,* 1997). To investigate the activity of the MHV-JHM 3Cpro, the predicted protease domain along with the full-length flanking hydrophobic domains (MP1 and MP2, membrane proteins 1 and 2) were cloned into the *in vitro* expression vector pET-11d under T7 promoter control and tested for protease activity in the presence and absence of membranes. A mutant 3Cpro construct was generated by polymerase chain reaction (PCR) mutagenesis, resulting in a substitution of the catalytic cysteine residue with an arginine residue (Table 1). Both wild type and mutant 3Cpro constructs were cotranscribed/translated *in vitro* with [^{35}S]methionine in the absence and presence of CMMs, and equal TCA-precipitable counts of each reaction were analyzed by SDS–PAGE and autoradiography (Fig. 6). Comparison of lanes 1 and 2 from this experiment indicates that the p27 cleavage product (3Cpro) is generated more efficiently from the 91 kDa translation product in the presence of CMMs (Fig. 6, lane 2). This may be due to an effect of membranes on the conformation of the proteinase itself or to an alteration in accessibility of the cleavage sites. Longer exposures of the gel in Fig. 6 show small quantities of p27 generated in the absence of membranes, in lane 1 (data not shown). As expected, pET-mut3Cpro does not generate p27 in the absence or presence of membranes (lanes 3 and 4). These results are consistent with the observations of Piñón et al. (1997) in that 3C processing events specifically leading to the release of p27 *in vitro* can occur in the absence of exogenously added membranes, but that they are greatly enhanced in the presence of CMMs. Finally, these data support the hypothesis that 3Cpro likely needs to be associated with intracellular membranes for efficient activity during virus infection.

DISCUSSION

Here we report the identification of six MHV-JHM gene 1 products, p250, p210, p40, p150, p27, and p15, which, together with the previously described products p28, p72, and p65, span the entire 4474 amino acids encoded by ORF1a (Table 3). Based on apparent molecular masses of proteins identified by immunoprecipitation using antisera generated to ORF1a fusion proteins, as well as the known location of each fusion protein epitope, we deduced that the ORF1a polyprotein is initially cleaved to generate four products, p28, p72, p250, and p150 (Fig. 7). P28, the amino-terminal cleavage product, is rapidly cleaved and is stable for at least 90 min after processing (Baker *et al.,* 1989; Denison and Perlman, 1986; Gao *et al.,* 1996). P72, p250, and p150 represent intermediates in the proteolytic processing of

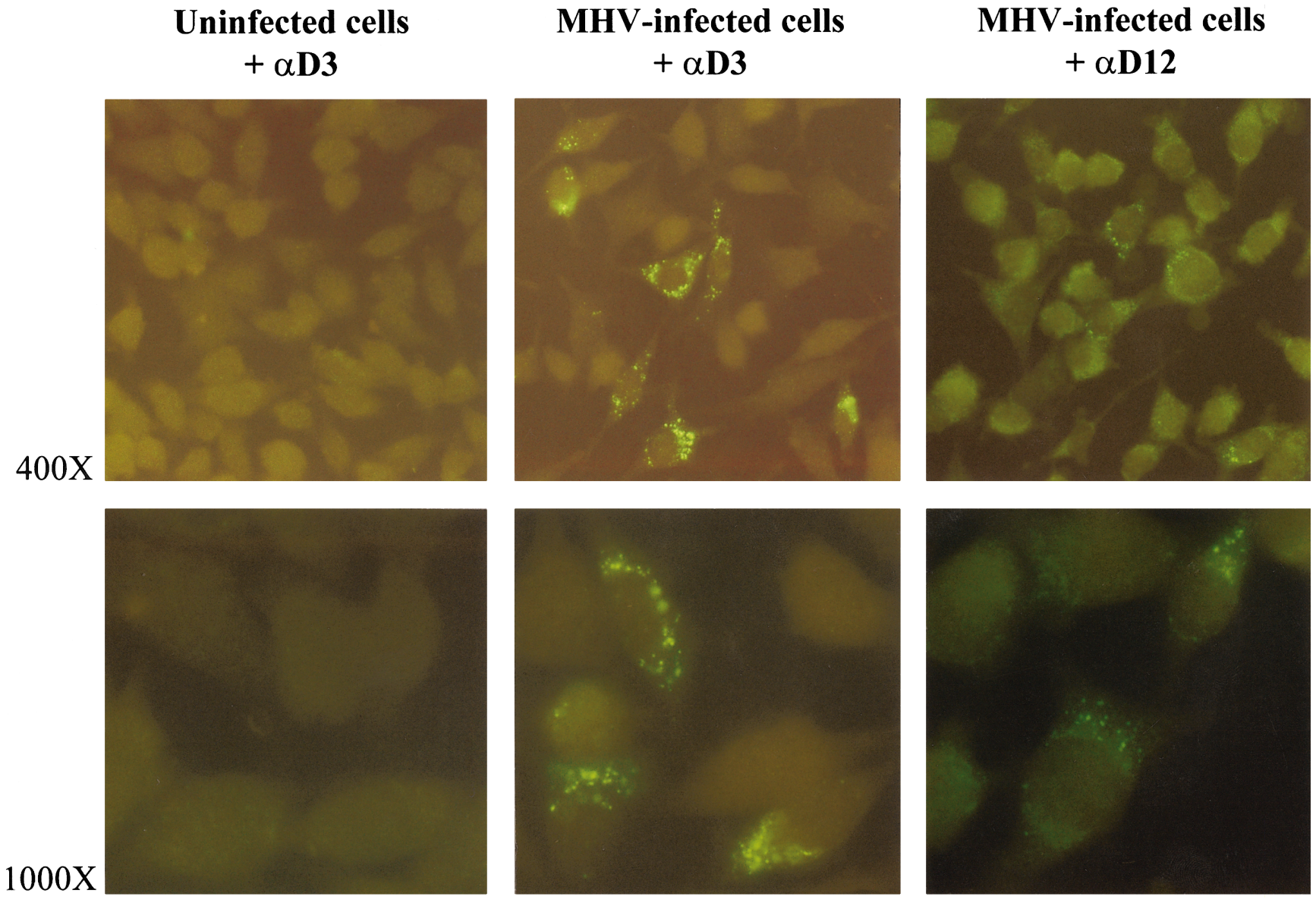

FIG. 5. Detection of MHV-JHM ORF1a proteins by immunofluorescence. DBT cells were infected with MHV-JHM and processed for immunofluorescence at 5.5 h p.i. as described under Materials and Methods. Antisera D3 and D12 detected ORF1a gene products in discrete punctate sites in the perinuclear region of infected cells. Typical fields are shown at 400× and 1000× magnification.

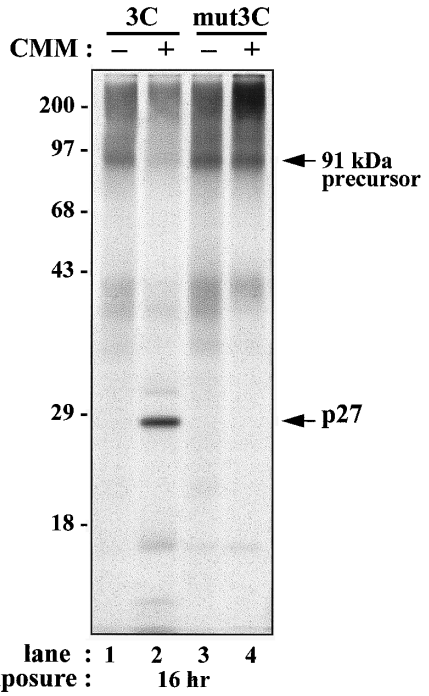

FIG. 6. Effect of membranes on 3Cpro proteolytic activity. *In vitro* cotranscription/translation was performed in rabbit reticulocyte lysates using the TNT expression system (as described under Materials and Methods), in the absence (−) and presence (+) of canine microsomal membranes (CMMs), as indicated for each lane. Equal TCA precipitable counts were analyzed by 12.5% SDS–PAGE and fluorography. The uncleaved 91-kDa precursor and 27-kDa product (likely representing aa 3337–3639 of the 3Cpro domain) are indicated. Molecular mass markers are shown on the left of the gel, and exposure length is indicated below.

ORF1a. P72 is processed to p65 (Gao *et al.,* 1996, and Fig. 1D). P250 is processed to p210 and p40, with p40 likely representing the carboxy-terminal cleavage product of p250 (Figs. 1 and 4). P150, which represents the carboxy-terminal region of ORF1a, is processed to p27, the MHV-JHM 3C-like proteinase, and p15 (Fig. 3). P150 is likely processed into several additional products as well.

Direct comparisons of MHV-JHM and A59 ORF1a gene products identified to date suggest that there may be one or more processing events unique to each strain. To determine if the high molecular mass JHM ORF1a products p250 and p210 identified here are distinct from previously described high molecular mass A59 products p290 and p240 (Denison *et al.,* 1992, 1995), we directly compared anti-D3 immunoprecipitations from radiolabeled JHM and A59 lysates (Fig. 2). Identical rates of migration by SDS–PAGE suggest that the two proteins, which under these conditions migrate with apparent molecular masses of 250 and 210 kDa, likely represent comparable regions of ORF1a from both strains. A processing event which is unique is the generation of p72 in the MHV-JHM strain. Immunoprecipitation of JHM and A59 lysates with anti-D3 (Fig. 2A) and anti-647 sera (H. Q. Gao and S. C. Baker, unpublished observations) demonstrated that the p72 protein is unique to the JHM strain. This is likely due to the presence of a putative PCP-1 cleavage site in the JHM strain that is not conserved in the A59 strain (Fig. 2B).

We show that the MHV-JHM ORF1a polyprotein is cleaved into at least 10 intermediates and protein prod-

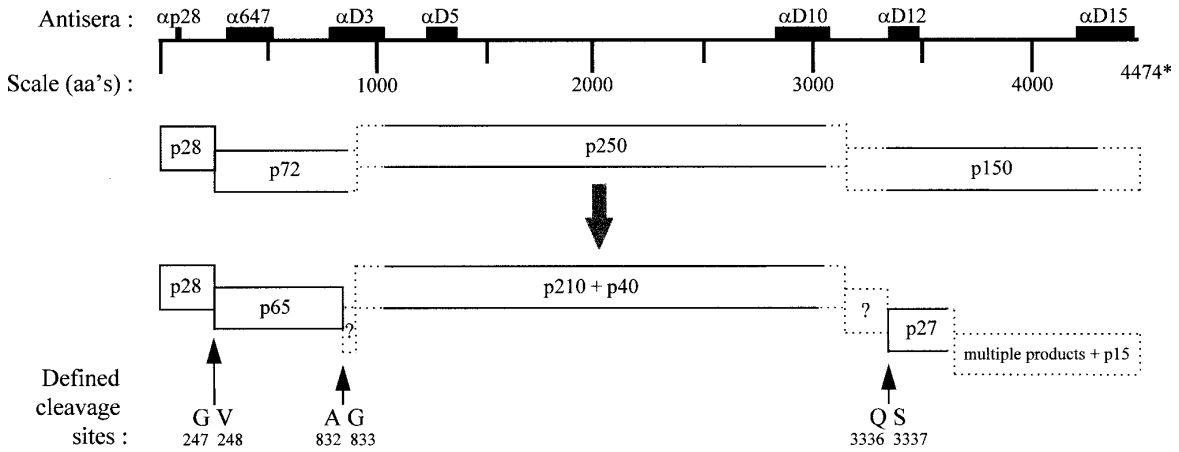

FIG. 7. Schematic representation of MHV-JHM ORF1a processing products. The 4474-amino-acid-long ORF1a polyprotein is cleaved to generate a series of intermediates and products depicted here, reflecting results described in this paper. Fusion protein domains used to generate antisera and detect cleavage products are depicted on the amino acid scale at the top. MHV-JHM ORF1a cleavage products are depicted with the observed molecular mass of each protein shown inside each box. Viral proteins labeled 6.0–6.5 h p.i. cleave rapidly to generate p28 and the downstream intermediates p72, p250, and p150. Intermediates are processed at varying rates to generate products p65, p210, p40, p27, and p15, all of which remain stable during a 180-min chase period. The three previously defined cleavage sites at the carboxy-terminus of p28, the carboxy-terminus of p65, and the amino-terminus of 3Cpro (p27) are shown. The G/V and A/G cleavage events are mediated by PCP-1, and the Q/S cleavage is mediated by 3Cpro. The exact amino- and carboxy-termini of all other proteins have not yet been determined, as depicted by the dotted lines. The location of the internal cleavage of p250 which results in the generation of p210 and p40 has not been definitively determined. Question marks indicate putative products that remain to be identified.

ucts, and clearly more products await identification. The proteolytic pathway used to generate these protein products is being actively investigated. To date, we know that the first papain-like cysteine proteinase (PCP-1) cleaves at G/V and A/G sites to generate p28 and p65, respectively (Bonilla *et al.,* 1997; Dong and Baker, 1994; Hughes *et al.,* 1995). Based on the size estimates of the cleavage products identified here and an analysis of potential cleavage sites, we speculate that PCP-1 (or potentially the PCP-2 domain located downstream of PCP-1) is responsible for cleavage of p72 and p250. Putative cleavage sites and size estimates of the resulting protein products are listed in Table 3. The relative positions of p210 and p40 are currently unclear since neither anti-D3 nor anti-D10 serum specifically immunoprecipitates p40. Because the D3 antigen encompasses only the amino terminal 14.2 kDa of p250 and the anti-D3 antiserum detects both p250 and p210, it is likely that p250 and p210 are co-amino-terminal. However, if p250 and p210 are co-amino-terminal, the D10 antiserum should encompass regions of both p210 and p40. It is currently unclear why we are unable to specifically precipitate p40 with any antiserum.

The proteolytic processing of the Nidovirus polymerases appears to be quite complex, requiring multiple proteinases and generating multiple intermediates. For the best studied Nidovirus, EAV, the 1727-aa (187-kDa) ORF1a polyprotein is cleaved into at least eight protein products (nsp1–8) by three distinct viral proteinases. Furthermore, alternative (and likely mutually exclusive) major and minor processing pathways for the EAV ORF1a polyprotein have been proposed (Wassenaar *et al.,* 1997). In addition, provisional mapping of the EAV ORF1b polyprotein suggests that there are at least four ultimate ORF1b cleavage products. However, since proteolytic processing of the EAV ORF1b polyprotein occurs quite slowly, a number of intermediates are also present in EAV-infected cells (van Dinten *et al.,* 1996). These findings illustrate the complexity of Nidovirus replicase complexes.

It is likely that some of the intermediates generated during processing of the MHV gene 1 polyprotein mediate functions distinct from those of the final processed products. The cleavage of p250 to p210 and p40 occurs relatively slowly in infected cells, with p250 still detectable 120 min after pulse labeling (Fig. 1). It is possible that MHV replicase complexes consisting of differentially processed ORF1a products are present in infected cells and exert distinct functions on viral RNA synthesis. In the Sindbis virus system it has been shown that replication of the viral RNA to negative sense and back to positive sense transcripts is regulated by differential processing of a nonstructural protein precursor P123 (de Groot *et al.,* 1990; Lemm and Rice, 1993; Shirako and Strauss, 1994). Early after Sindbis virus infection, P123 together with nsP4 forms the negative strand replication complex. In contrast, late in infection after the viral nsP2 proteinase has accumulated to significant levels, fully processed nsP1, nsP2, nsP3, and nsP4 form the positive strand replication complex and shift viral RNA synthesis from the production of negative strand templates to the production of genome-sense transcripts. Similar to Sindbis virus, the coronavirus replicase contains numerous cleavage sites and several proteinase domains responsible for processing the large replicase polyprotein. Accumulation of the viral PCP-1 and 3Cpro proteinases during the course of infection very likely alters the kinetics of *trans*-cleavage events and the stability of the p72, p250, and p150 processing intermediates which may play distinct regulatory roles in coronavirus genome replication.

Membrane association of many positive-strand RNA virus replication complexes has been described in the literature (Bienz *et al.,* 1994; Chambers *et al.,* 1990; Froshauer *et al.,* 1988; van Dinten *et al.,* 1996). Due to the presence of predicted hydrophobic stretches within the MHV gene 1 polyprotein (Gorbalenya *et al.,* 1989; Lee *et al.,* 1991), it is thought that some of the mature gene 1 products may be transmembrane proteins which serve to anchor the viral replicase complex to membranes via protein–protein interactions. In this report, we demonstrate that the MHV-JHM ORF1a proteolytic products are present as a complex in virus-infected cells. When infected cells are disrupted by mild detergent (0.5% NP-40), protein complexes are precipitated with ORF1a antisera (Fig. 4). These complexes consist of: a high-molecular-weight protein (>300 kDa) which we speculate extends from ORF1a into ORF1b by ribosomal frameshifting during translation; p250, p210, and p40 which represent the central domain of ORF1a and include the two papain-like cysteine proteinases, PCP-1 and PCP-2; and p150, which represents the carboxy-terminal portion of ORF1a and includes the 3C-like proteinase. Intracellular immunofluorescence analysis revealed that this complex localizes to the perinuclear region, likely the endoplasmic reticulum or intermediate compartment (Fig. 5). Replicase complex formation and ER localization has also been reported for the EAV replicase (Snijder *et al.,* 1994; van Dinten *et al.,* 1996). Similarly, one MHV-A59 ORF1a product has been localized to the Golgi apparatus by immunofluorescent staining (Bi *et al.,* 1995). It is interesting to note that although EAV ORF1b products localize to membranes, the only hydrophobic, potentially membrane-spanning regions of gene 1 are found within ORF1a surrounding the viral 3C-like nsp4 protease domain (Snijder *et al.,* 1994). Additionally, EAV ORF1a proteins have been shown to coimmunoprecipitate with ORF1b-specific antisera (van Dinten *et al.,* 1996), suggesting strong protein–protein interactions between the cleaved gene 1 products *in vivo.*

For the MHV replicase, the two regions flanking the 3Cpro, termed MP1 and MP2, are likely transmembrane

domains which may direct the precursor polyprotein to intracellular membranes. For MHV-A59 it has been shown that the hydrophobic domains flanking 3Cpro associate with membrane fractions of *in vitro* translation reactions (Piñón *et al.,* 1997). Even after proteolytic processing, these transmembrane domains may anchor 3Cpro and other ORF1a/ORF1b proteins to membranes by strong protein–protein interactions. The results of Piñón *et al.* (1997) demonstrated that addition of membranes to an *in vitro* transcription/translation reaction significantly increased the efficiency of 3Cpro cleavage from flanking hydrophobic regions. Similarly, we found that addition of canine microsomal membranes to *in vitro* transcription/translation reactions of an MHV-JHM 3Cpro precursor dramatically enhanced the efficiency of the processing events, generating a p27 (3Cpro catalytic core; Fig. 6). These results are consistent with the hypothesis that membrane association of 3Cpro *in vivo* is probably necessary for it to adopt a proteolytically efficient conformation and that the regions surrounding this domain are responsible for mediating its membrane association.

Taken together, these data imply that Nidovirus gene 1 cleavage products assemble into a large replication complex that is anchored to membranes by protein–protein interactions with the hydrophobic ORF1a product(s). Future studies are aimed at determining if altered proteolytic processing or assembly of the replicase complex affects viral RNA synthesis.

MATERIALS AND METHODS

Virus and cells

Plaque-cloned MHV strains JHM (Makino *et al.,* 1984) and A59 (Lai and Stohlman, 1981) were used throughout this study. Gene 1 of both strains has been completely cloned and sequenced (Lee *et al.,* 1991, as modified by Bonilla *et al.,* 1994 for MHV-JHM; Bredenbeek *et al.,* 1990, and Bonilla *et al.,* 1994, for MHV-A59). The viruses were propagated on DBT cells (Hirano *et al.,* 1974) maintained in Dulbecco's modified eagle medium supplemented with 5% fetal calf serum (FCS), 10% tryptone phosphate broth, 2% penicillin/streptomycin, and 2% L-glutamine (all tissue culture reagents were from Gibco-BRL, Gaithersberg, MD).

Generation of rabbit antisera to MHV-JHM ORF1a regions

A panel of antisera directed against specific domains of MHV-JHM ORF1a was generated using the overall strategy of reverse transcription and polymerase chain reaction (RT-PCR) amplification of a region of interest, cloning and expression of the region as a GST-fusion protein, purification of the GST-ORF1a fusion protein, and injection of the purified fusion protein into rabbits. Briefly, DBT cells were infected with MHV-JHM at a multiplicity of infection (m.o.i.) of 5. RNA was isolated from the cells at 12–13 h postinfection (p.i.) using RNAzol B according to manufacturer's instructions (Tel-test, Inc., Friendswood, TX). cDNA was generated by first denaturing 0.1 μg RNA with 18 mM methyl mercury hydroxide for 5 min at room temperature. The RNA was then incubated for 2 h at 42°C in a reaction mixture containing the following: 0.07 M β-mercaptoethanol, 0.1 μg random hexamer oligonucleotide primers, 10 μM each deoxyribonucleoside triphosphate, 85 mM Tris–HCl, pH 8.3, 34 mM KCl, 8.5 mM $MgCl_2$, 40 U of RNAsin and 8 U of avian myeloblastosis virus reverse transcriptase (Seikagaku America, Inc., Rockville, MD). The cDNA synthesis reaction was terminated by heat inactivation at 95°C for 3 min, and then quickly cooled on ice.

Regions of interest were amplified from the cDNA using specific primers (Table 1). Each PCR reaction contained approximately 30 ng of cDNA, 0.4 μM each primer, 0.25 mM each dNTP, 1 μl Advantage KlenTaq Polymerase Mix, and 10× PCR reaction buffer (Clontech, Palo Alto, CA) in a total reaction volume of 50 μl. Amplification conditions consisted of 35 cycles of: 94°C for 2 s, 50°C for 30 s, and 68°C for 1 min. Each PCR product was digested with restriction enzymes and ligated into the *Xba*I and *Hin*dIII sites of the bacterial expression vector pGEX-KG (kindly provided by Dr. Steven Broyles, Indiana University). Following transformation of the ligation reaction into *Escherichia coli* DH5 alpha cells, ampicillin-resistant bacteria were induced for fusion protein production using the method of Guan and Dixon (1991). Briefly, bacteria were grown at 30°C in 2× YT containing 50 μg/ml ampicillin until cultures reached an OD_{600} of 0.5–0.55. Fusion proteins were then induced by the addition of IPTG, as optimized for each transformant: 50 μM IPTG for 1 h (D5, D12, and D15), 50 μM IPTG for 2 h (D10), or 100 μM IPTG for 2 h (D3). Cells were harvested by centrifugation (3000 g). The bacteria from 1 l of culture was resuspended in 100 ml PBS and lysed by sonication. Fusion proteins were isolated from the soluble fraction by affinity chromatography over glutathione–sepharose bead columns as described by the manufacturer (Pharmacia Biotech, Piscataway, NJ). The fusion proteins were eluted by competition with 20 mM glutathione in 120 mM NaCl and 100 mM Tris–HCl, pH 8.0. The yield per liter of culture varied greatly, ranging from 400 μg to 7 mg, depending on the apparent solubility of each fusion protein. Approximate yields of purified protein were as follows: D3, 7.0 mg/l; D5, 970 μg/l; D10, 800 μg/l; D12, 400 μg/l, and D15, 2.5 mg/l. Rabbits were injected intramuscularly and subcutaneously with 1 ml of 200–500 μg protein emulsified in 1 ml of Freund's adjuvant (complete adjuvant for first injection; incomplete for two or three subsequent in-

jections, each approximately 30 days apart). Immune sera were collected 10–14 days following each injection.

Preparation of radiolabeled whole cell lysates

Monolayers of 80–100% confluent DBT cells in 100 mm petri dishes were infected with MHV-JHM at an m.o.i. of 5–10 plaque-forming units/cell for 1 h, and then incubated at 37°C in supplemented media containing 4 μg/ml Actinomycin D for an additional 4.5 h. At 5.5 h p.i. media were replaced with MEM lacking methionine for 30 min. Proteins were metabolically radiolabeled with [^{35}S]methionine (100 μCi/ml; ICN, Costa Mesa, CA) for 90 min, unless indicated otherwise in the text. For direct labeling experiments, cells were washed following labeling with cold PBS on ice and lysed in 300 μl of either lysis buffer A or B (see below). For pulse–chase experiments, cells in 60-mm dishes were labeled for 30 min, washed twice with supplemented MEM, and incubated with media containing a 10-fold excess of methionine (3 mM) and cysteine (4 mM) for the chase periods. At the times p.i. indicated in the text for each experiment, one plate of cells was washed with cold PBS on ice and lysed in 150 μl of lysis buffer A. Lysis buffer A contained 4% SDS, 3% DTT, 40% glycerol, and 0.0625 M Tris, pH 6.8 (as previously described, Baker *et al.,* 1989). Lysates prepared in buffer A were passed through a 22-gauge needle to shear chromosomal DNA and either used directly or frozen at −80°C. Lysis buffer B contained 100 mM NaCl, 10 mM Tris–HCl, pH 7.5, 1 mM EDTA, 0.5% NP-40, 0.1 mM PMSF, and 0.3 TIU/ml aprotinin. Lysates prepared in buffer B were solubilized by pipetting, nuclei pelleted by centrifugation for 5 min at 8000 rpm, and the postnuclear supernatants harvested and either used directly or frozen at −80°C.

Immunoprecipitation of MHV-JHM ORF1a proteins

Virus-encoded polyproteins expressed during infection of DBT cells were identified by immunoprecipitation from whole cell lysates prepared as described above. Lysates from about 1×10^6 cells were immunoprecipitated with 5–10 μl of antisera in a total volume of 1 ml RIPA buffer (0.5% Triton X-100, 0.1% SDS, 300 mM NaCl, 50 mM Tris–HCl, pH 7.4, 4 mM EDTA). Antibody–antigen complexes were precipitated by addition of 40 μl of a 1:1 suspension of protein A–Sepharose CL4B beads (Pharmacia Biotech, Piscataway, NJ) in RIPA buffer. Antibody–antigen complexes were washed one time with 1 ml RIPA buffer, and then incubated 30 min at 37°C or boiled for 3 min in 30 μl of Laemmli 2× sample buffer (Laemmli, 1970). Proteins were electrophoresed on 15% polyacrylamide gels containing 0.1% sodium dodecyl sulfate (SDS–PAGE gels) or 5–15% gradient SDS–PAGE gels, as indicated in the text. Following electrophoresis, gels were fixed in 25% methanol and 10% acetic acid, enhanced with Entensify A and B (NEN Research Products, Boston, MA), dried, and exposed to Kodak X-ray film at −80°C.

Molecular mass estimates of MHV-JHM ORF1a products

For molecular mass determinations, immunoprecipitated products were electrophoresed on 5 and 7.5% SDS–PAGE gels along with three standards: See Blue, which contains a 250-kDa protein (Novex, San Diego, CA), Bench Mark, and a ^{14}C high molecular weight standard (Gibco BRL, Gaithersburg, MD). Estimates of molecular mass of ORF1a products were calculated from regression curves of log molecular weight vs. relative mobility (R_f) established using the standards.

Immunofluorescence detection of MHV-JHM ORF1a proteins

Monolayers of 5.0×10^4 DBT cells in eight-well chamber slides were infected with MHV-JHM at an m.o.i. of 10 and incubated at 37°C. At 5.0–5.5 h p.i., the cells were washed two times with PBS and fixed with 3.7% formaldehyde in PBS for 30 min. The fixed cells were washed three times with PBS containing 10 mM glycine, permeabilized with 0.1% Triton X-100 for 10 min, and then washed three times with PBS containing 10 mM glycine. The fixed cells were incubated overnight with 1:2000–1:3500 dilutions of the designated primary rabbit antisera in PBS, 5% FCS, and 0.3% saponin (ICN, Cleveland, OH) at 4°C in a moist chamber. Following this incubation, cells were washed with PBS and 0.03% saponin for 1 h, and then incubated with FITC-conjugated donkey anti-rabbit IgG (Jackson ImmunoResearch Laboratories, West Grove, PA) at a dilution of 1:200 in PBS, 5% FCS, 0.3% saponin, and 0.001% DAPI (4,′6-diamidino-2-phenylindole; Sigma, St. Louis, MO) at 37°C for 1 h. The cells were then washed with PBS and 0.03% saponin for 1 h and mounted with 50% glycerol and glass coverslips. The cells were examined under a fluorescence microscope (Nikon) and photographed using Fuji (ASA 800) color print film.

In vitro cloning and expression of the MHV-JHM 3C-like proteinase domain

The 3C proteinase domain was RT-PCR amplified as described above using the primers indicated in Table 1. The forward PCR primer was designed with an ATG start codon in good Kozak consensus sequence (Kozak, 1989), and the reverse primer was designed with an in-frame stop codon. The PCR product was digested with *Xba*I and *Eco*RI and directionally cloned into plasmid pET-11d (Novagen, Madison, WI) under the control of a T7 promoter and lac operator. This plasmid was designated pET-3Cpro. To generate the mutant 3Cpro expression construct, the *Bam*HI–*Eco*RI fragment of pET-3Cpro was

replaced with a fragment generated by PCR using primers B153 and B158 (Table 1), which encodes an arginine instead of a cysteine at position 3481. The resultant plasmid was designated pET-mut3Cpro. The catalytic regions of pET-3Cpro and pET-mut3Cpro were confirmed by dideoxy sequencing (Sequenase DNA sequencing kit, Version 2.0; U. S. Biochemicals, Cleveland, OH) using primer B169 (5′-CATACAATGGCAGACCC-3′), which binds nucleotides 10572–10588 of MHV-JHM ORF1a (numbered according to Lee *et al.,* 1991, as modified by Bonilla *et al.,* 1994).

Plasmid DNAs were cotranscribed and translated in rabbit reticulocyte lysates (TNT lysates; Promega Biotech, Madison, WI) according to the manufacturer's instructions. Reactions were performed in a total volume of 12.5 μl using approximately 1 μg of supercoiled plasmid DNA and 10 μCi of [^{35}S]methionine (ICN Biomed., Costa Mesa, CA), and incubated at 30°C for 90 min. [^{35}S]Methionine incorporation into the translation products was quantitated by trichloroacetic acid (TCA) precipitation (Maniatis *et al.,* 1982). Equal TCA-precipitable counts (50,000 cpm) of each protein product were mixed with Laemmli 2× sample buffer, boiled 3 min, analyzed by gel electrophoresis in 12.5% SDS–PAGE gels, and visualized by fluorography, as described above.

ACKNOWLEDGMENTS

We thank David Axtell for his assistance in the production of several GST-fusion proteins, John Zaryczny for his assistance with rabbit injections and sera collection, and Dr. Phong Le for advice on immunofluorescence studies. This research was supported by Public Health Service Research Grant AI 32065 from the National Institutes of Health.

REFERENCES

Baker, S. C., Shieh, C. K., Soe, L. H., Chang, M. F., Vannier, D. M., and Lai, M. M. (1989). Identification of a domain required for autoproteolytic cleavage of murine coronavirus gene A polyprotein. *J. Virol.* 63, 3693–3699.

Baker, S. C., Yokomori, K., Dong, S., Carlisle, R., Gorbalenya, A. E., Koonin, E. V., and Lai, M. M. (1993). Identification of the catalytic sites of a papain-like cysteine proteinase of murine coronavirus. *J. Virol.* 67, 6056–6063.

Baric, R. S., Stohlman, S. A., and Lai, M. M. (1983). Characterization of replicative intermediate RNA of mouse hepatitis virus: Presence of leader RNA sequences on nascent chains. *J. Virol.* 48, 633–640.

Bi, W., Bonilla, P. J., Holmes, K. V., Weiss, S. R., and Leibowitz, J. L. (1995). Intracellular localization of polypeptides encoded in mouse hepatitis virus open reading frame 1A. *Adv. Exp. Med. Biol.* 380, 251–258.

Bienz, K., Egger, D., and Pfister, T. (1994). Characteristics of the poliovirus replication complex. *Arch. Virol. (Suppl.)* 9, 147–157.

Bonilla, P. J., Gorbalenya, A. E., and Weiss, S. R. (1994). Mouse hepatitis virus strain A59 RNA polymerase gene ORF 1a: Heterogeneity among MHV strains. *Virology* 198, 736–740.

Bonilla, P. J., Hughes, S. A., and Weiss, S. R. (1997). Characterization of a second cleavage site and demonstration of activity in trans by the papain-like proteinase of the murine coronavirus mouse hepatitis virus strain A59. *J. Virol.* 71, 900–909.

Boursnell, M. E., Brown, T. D., Foulds, I. J., Green, P. F., Tomley, F. M., and Binns, M. M. (1987). Completion of the sequence of the genome of the coronavirus avian infectious bronchitis virus. *J. Gen. Virol.* 68, 57–77.

Bredenbeek, P. J., Pachuk, C. J., Noten, A. F. H., Charite, J., Luytjes, W., Weiss, S. R., and Spaan, W. J. M. (1990). The primary structure and expression of the second open reading frame of the polymerase gene of the coronavirus MHV-A59: A highly conserved polymerase is expressed by an efficient ribosomal frameshifting mechanism. *Nucl. Acids Res.* 18, 1825–1832.

Brierley, I., Boursnell, M. E., Binns, M. M., Bilimoria, B., Blok, V. C., Brown, T. D., and Inglis, S. C. (1987). An efficient ribosomal frameshifting signal in the polymerase-encoding region of the coronavirus IBV. *EMBO J.* 6, 3779–3785.

Cavanagh, D. (1997). Nidovirales: A new order comprising Coronaviridae and Arteriviridae. *Arch. Virol.* 142, 629–633.

Chambers, T. J., Hahn, C. S., Galler, R., and Rice, C. M. (1990). Flavivirus genome organization, expression, and replication. *Annu. Rev. Microbiol.* 44, 649–688.

de Groot, R. J., Hardy, W. R., Shirako, Y., and Strauss, J. H. (1990). Cleavage-site preferences of Sindbis virus polyproteins containing the non-structural proteinase. Evidence for temporal regulation of polyprotein processing in vivo. *EMBO J.* 9, 2631–2638.

Denison, M., and Perlman, S. (1987). Identification of putative polymerase gene product in cells infected with murine coronavirus A59. *Virology* 157, 565–568.

Denison, M. R., Hughes, S. A., and Weiss, S. R. (1995). Identification and characterization of a 65-kDa protein processed from the gene 1 polyprotein of the murine coronavirus MHV-A59. *Virology* 207, 316–320.

Denison, M. R., and Perlman, S. (1986). Translation and processing of mouse hepatitis virus virion RNA in a cell-free system. *J. Virol.* 60, 12–18.

Denison, M. R., Zoltick, P. W., Hughes, S. A., Giangreco, B., Olson, A. L., Perlman, S., Leibowitz, J. L., and Weiss, S. R. (1992). Intracellular processing of the N-terminal ORF 1a proteins of the coronavirus MHV-A59 requires multiple proteolytic events. *Virology* 189, 274–284.

de Vries, A. A. F., Horzinek, M. C., Rottier, P. J. M., and de Groot, R. J. (1997). The genome organization of the Nidovirales: Similarities and differences between Arteri-, Toro-, and Coronaviruses. *Semin. Virol.* 8, 33–47.

Dong, S., and Baker, S. C. (1994). Determinants of the p28 cleavage site recognized by the first papain-like cysteine proteinase of murine coronavirus. *Virology* 204, 541–549.

Eleouet, J. F., Rasschaert, D., Lambert, P., Levy, L., Vende, P., and Laude, H. (1995). Complete sequence (20 kilobases) of the polyprotein-encoding gene 1 of transmissible gastroenteritis virus. *Virology* 206, 817–822.

Froshauer, S., Kartenbeck, J., and Helenius, A. (1988). Alphavirus RNA replicase is located on the cytoplasmic surface of endosomes and lysosomes. *J. Cell Biol.* 107, 2075–2086.

Gao, H. Q., Schiller, J. J., and Baker, S. C. (1996). Identification of the polymerase polyprotein products p72 and p65 of the murine coronavirus MHV-JHM. *Virus Res.* 45, 101–109.

Gorbalenya, A. E., Koonin, E. V., Donchenko, A. P., and Blinov, V. M. (1989). Coronavirus genome: prediction of putative functional domains in the non-structural polyprotein by comparative amino acid sequence analysis. *Nucl. Acids Res.* 17, 4847–4861.

Guan, K. L., and Dixon, J. E. (1991). Eukaryotic proteins expressed in Escherichia coli: an improved thrombin cleavage and purification procedure of fusion proteins with glutathione S-transferase. *Anal. Biochem.* 192, 262–267.

Herold, J., Raabe, T., Schelle-Prinz, B., and Siddell, S. G. (1993). Nucleotide sequence of the human coronavirus 229E RNA polymerase locus. *Virology* 195, 680–691.

Hirano, N., Fujiwara, K., Hino, S., and Matumoto, M. (1974). Replication and plaque formation of mouse hepatitis virus (MHV-2) in mouse cell line DBT culture. *Arch. Gesam. Virusforsch.* 44, 298–302.

Hughes, S. A., Bonilla, P. J., and Weiss, S. R. (1995). Identification of the murine coronavirus p28 cleavage site. *J. Virol.* 69, 809–813.

Jeong, Y. S., and Makino, S. (1994). Evidence for coronavirus discontinuous transcription. *J. Virol.* 68, 2615–2623.

Kozak, M. (1989). The scanning model for translation: An update. *J. Cell Biol,* 108, 229–241.

Laemmli, U. K. (1970). Cleavage of structural proteins during the assembly of the head of bacteriophage T4. *Nature* 227, 680–685.

Lai, M. M., Liao, C. L., Lin, Y. J., and Zhang, X. (1994). Coronavirus: How a large RNA viral genome is replicated and transcribed. *Infect. Agents Dis.* 3, 98–105.

Lai, M. M. C., and Stohlman, S. A. (1981). Comparative analysis of RNA genomes of mousehepatitis viruses. *J. Virol,* 38, 661–670.

Lee, H. J., Shieh, C. K., Gorbalenya, A. E., Koonin, E. V., La Monica, N., Tuler, J., Bagdzhadzhyan, A., and Lai, M. M. (1991). The complete sequence (22 kilobases) of murine coronavirus gene 1 encoding the putative proteases and RNA polymerase. *Virology* 180, 567–582.

Lemm, J. A., and Rice, C. M. (1993). Roles of nonstructural polyproteins and cleavage products in regulating Sindbis virus RNA replication and transcription. *J. Virol.* 67, 1916–1926.

Liu, D. X., and Brown, T. D. (1995). Characterisation and mutational analysis of an ORF 1a-encoding proteinase domain responsible for proteolytic processing of the infectious bronchitis virus 1a/1b polyprotein. *Virology* 209, 420–427.

Lu, X., Lu, Y., and Denison, M. R. (1996). Intracellular and in vitro-translated 27-kDa proteins contain the 3C-like proteinase activity of the coronavirus MHV-A59. *Virology* 222, 375–382.

Lu, Y., and Denison, M. R. (1997). Determinants of mouse hepatitis virus 3C-like proteinase activity. *Virology* 230, 335–342.

Lu, Y., Lu, X., and Denison, M. R. (1995). Identification and characterization of a serine-like proteinase of the murine coronavirus MHV-A59. *J. Virol.* 69, 3554–3559.

Makino, S., Taguchi, F., Hirano, N., and Fujiwara, K. (1984). Analysis of genomic and intracellular viral RNAs of small plaque mutants of mouse hepatitis virus, JHM strain. *Virology* 139, 9–17.

Maniatis, T. E., Fritsch, E. F., and Sambrook, J. (1982). "Molecular Cloning: A Laboratory Manual." Cold Spring Harbor Laboratory, Cold Spring Harbor, NY.

Pachuk, C. J., Bredenbeek, P. J., Zoltick, P. W., Spaan, W. J., and Weiss, S. R. (1989). Molecular cloning of the gene encoding the putative polymerase of mouse hepatitis coronavirus, strain A59. *Virology* 171, 141–148.

Piñón, J. D., Mayreddy, R. R., Turner, J. D., Khan, F. S., Bonilla, P. J., and Weiss, S. R. (1997). Efficient autoproteolytic processing of the MHV-A59 3C-like proteinase from the flanking hydrophobic domains requires membranes. *Virology* 230, 309–322.

Sawicki, S. G., and Sawicki, D. L. (1990). Coronavirus transcription: Subgenomic mouse hepatitis virus replicative intermediates function in RNA synthesis. *J. Virol.* 64, 1050–1056.

Sethna, P. B., Hung, S. L., and Brian, D. A. (1989). Coronavirus subgenomic minus-strand RNAs and the potential for mRNA replicons. *Proc. Natl. Acad. Sci. USA* 86, 5626–5630.

Seybert, A., Ziebuhr, J., and Siddell, S. G. (1997). Expression and characterization of a recombinant murine coronavirus 3C-like proteinase. *J. Gen. Virol.* 78, 71–75.

Shirako, Y., and Strauss, J. H. (1994). Regulation of Sindbis virus RNA replication: uncleaved P123 and nsP4 function in minus-strand RNA synthesis, whereas cleaved products from P123 are required for efficient plus-strand RNA synthesis. *J. Virol.* 68, 1874–1885.

Snijder, E. J., Wassenaar, A. L. M., and Spaan, W. J. M. (1994). Proteolytic processing of the replicase ORF1a protein of equine arteritis virus. *J. Virol.* 68, 5755–5764.

Spaan, W., Delius, H., Skinner, M., Armstrong, J., Rottier, P., Smeekens, S., van der Zeijst, B. A., and Siddell, S. G. (1983). Coronavirus mRNA synthesis involves fusion of noncontiguous sequences. *EMBO J.* 2, 1839–1844.

Tibbles, K. W., Brierley, I., Cavanagh, D., and Brown, T. D. (1996). Characterization in vitro of an autocatalytic processing activity associated with the predicted 3C-like proteinase domain of the coronavirus avian infectious bronchitis virus. *J. Virol.* 70, 1923–1930.

van der Most, R. G., and Spaan, W. J. M. (1995). Coronavirus replication, transcription, and RNA recombination. *In* "The Coronaviridae" (S. G. Siddell, Ed.), pp. 11–31. Plenum, New York.

van Dinten, L. C., Wassenaar, A. L., Gorbalenya, A. E., Spaan, W. J., and Snijder, E. J. (1996). Processing of the equine arteritis virus replicase ORF1b protein: Identification of cleavage products containing the putative viral polymerase and helicase domains. *J. Virol.* 70, 6625–6633.

van Marle, G., Luytjes, W., van der Most, R. G., van der Straaten, T., and Spaan, W. J. (1995). Regulation of coronavirus mRNA transcription. *J. Virol.* 69, 7851–7856.

Wassenaar, A. L. M., Spaan, W. J. M., Gorbalenya, A. E., and Snijder, E. J. (1997). Alternative proteolytic processing of the arterivirus replicase ORF1a polyprotein: Evidence that NSP2 acts as a cofactor for the NSP4 serine protease. *J. Virol.* 71, 9313–9322.

Zhang, X., and Lai, M. M. (1995). Interactions between the cytoplasmic proteins and the intergenic (promoter) sequence of mouse hepatitis virus RNA: Correlation with the amounts of subgenomic mRNA transcribed. *J. Virol.* 69, 1637–1644.

Ziebuhr, J., Herold, J., and Siddell, S. G. (1995). Characterization of a human coronavirus (strain 229E) 3C-like proteinase activity. *J. Virol.* 69, 4331–4338.